Macromolecules

pubs.acs.org/Macromolecules Article

Concentration Regimes for Extensional Relaxation Times of Unentangled Polymer Solutions

Diego D. Soetrisno, Carina D. V. Martínez Narváez, Vivek Sharma,* and Jacinta C. Conrad*

Cite This: *Macromolecules* 2023, 56, 4919−4928 Read Online

ACCESS | Metrics & More | Article Recommendations | Supporting Information

ABSTRACT: We study the extensional flow properties of polyacrylamide (PAM) solutions with various molecular weights and dispersities using a dripping-onto-substrate (DoS) protocol. A recent study [Dinic and Sharma, *Macromolecules* **2020**, *53*, 4821−4835] suggested that coil−stretch hysteresis, which occurs when the drag coefficient ratio of stretched and coiled polymer chains $\varsigma_s/\varsigma_c > 4.5$, controls the scaling exponent of the extensional relaxation time λ_E with concentration. Here, we test this hypothesis by varying ς_s/ς_c through the PAM molecular weight distribution. The scaling exponent of the concentration dependence of λ_E is $m = 0.34$ for PAM solutions with $\varsigma_s/\varsigma_c < 4.5$ and $m > 0.5$ for PAM solutions with $\varsigma_s/\varsigma_c > 4.5$. The increase in the scaling exponent is attributed to the presence of coil−stretch hysteresis, which screens the excluded volume interactions under extensional flow. For highly disperse solutions with $Đ \approx 21$, the transition from an exponent of 0.67 to 1 occurs at overlap concentration c^* derived from the weight-averaged molecular weight instead of viscosity-averaged molecular weight, highlighting the role of long chains. These results provide insight into the role of the polymer size distribution in the concentration-dependent extensional material response in dilute and unentangled semidilute solutions.

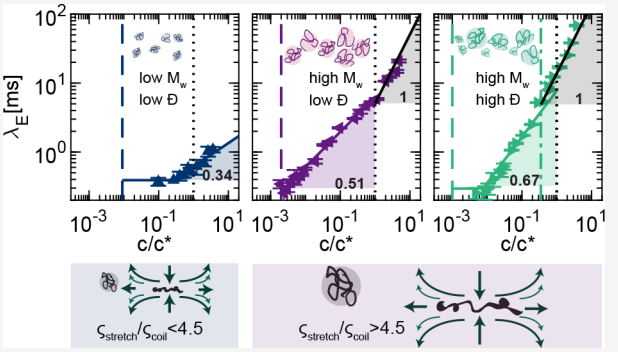

INTRODUCTION

Understanding the role of polymer concentration on the rheology of polymer solutions[1−6] is of great interest for applications such as electrospinning[7] and 3-D printing.[8] The concentration-dependent variation in the static and dynamic properties of macromolecules in solution depends on polymer−solvent interactions, polymer flexibility, and polymer molecular weight.[2,5,9] Under quiescent conditions, the volume available per coil in a polymer solution equals the unperturbed coil size at the so-called overlap concentration c^*. The different concentration regimes are determined by whether the polymer coils overlap with each other in the solution[1,2] and are typically divided into dilute ($c < c^*$), unentangled semidilute ($c^* < c < c_e$), and entangled ($c > c_e$) regimes,[1] where c_e is the entanglement concentration.[2,5]

In the dilute regime ($c < c^*$), the polymer coils do not overlap and the shear rheology is primarily determined by intrachain hydrodynamic interactions (HI) and excluded volume (EV) interactions. Both forces are modulated by polymer−solvent interactions as captured by Zimm theory[3] and not by interactions between the coils. HI and EV interactions are progressively screened in the semidilute regime ($c > c^*$), where blob models are used to describe the chain dynamics and shear rheology response. The effect of local interactions is included via the Zimm model for dynamics within a blob, whereas the global dynamics of an idealized chain of blobs is described using Rouse dynamics. The number and size of blobs are determined self-consistently for equilibrium, overlapping coils by using scaling theory.

In entangled solutions ($c > c_e$), the topological constraints or entanglements give rise to extremely slow chain dynamics. The diffusion coefficient D, zero-shear viscosity η_0, and shear relaxation time λ_s show distinct transitions at c^* and c_e as functions of concentration. Though the shear rheology response of unentangled polymer solutions exhibits universal characteristics,[2,5,9] the corresponding macromolecular parameters and shear rheological measures fail to capture the variation and range of effects that are present in processing.[10,11] These involve material performances commonly associated with jettability, sprayability, mist formation during coating, stringiness, and spinnability.

Processing operations and applications such as drop formation during jetting or spraying, fiber spinning, coating, and flow through porous media involve streamwise velocity gradients associated with extensional flows.[10−13] Macromolecules can undergo significantly higher degrees of

Received: January 17, 2023
Revised: May 31, 2023
Published: June 27, 2023

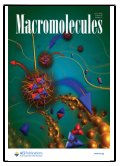

https://doi.org/10.1021/acs.macromol.3c00097
Macromolecules 2023, 56, 4919−4928

stretching and orientation in response to extensional flow, influencing their chain dynamics, the degree of overlap, and extensional relaxation time λ_E.[14] Unentangled solutions of flexible polymers often display strain hardening, and extensional viscosity η_E values can be several orders of magnitude higher than shear viscosity $\eta(\dot{\gamma})$, even though for Newtonian fluids $\eta_E = 3\eta$.

Polymer coils are only mildly perturbed in response to shear flow. It is well-established, however, that polymers can undergo significant stretching in response to extensional flow, leading to a coil−stretch transition beyond a critical extension rate $\dot{\epsilon}_{c\to s}$. Earlier studies in the 1970s postulated that the coil−stretch transition occurs in macromolecules if the ratio of deformation rate to the relaxation rate (of unperturbed coils, λ_s) exceeds 1/2.[1,15−17] Furthermore, theoreticians predicted the existence of coil−stretch hysteresis such that the prestretched chains relax back or undergo the stretch-coil transition $\dot{\epsilon}_{s\to c} < \dot{\epsilon}_{c\to s}$ (at a lower deformation rate). Work done decades after provided evidence for both the coil−stretch transition and hysteresis by visualizing conformation changes in fluorescently labeled DNA using precision microfluidics experiments.[18,19] Thereafter, several studies performed simulations to determine that coil−stretch hysteresis manifests if the ratio of drag coefficients of the stretched to unperturbed coils exceeds a critical value of $\zeta_s/\zeta_c > 4.5$.[18−22] Polymer chains exhibit entropic resistance to stretching, and conformation-dependent drag depends nonlinearly on the degree of stretching, deformation history, and initial conditions. Coil−stretch hysteresis arises as large polymer molecules can be kinetically trapped in either a coil or an extended state. The hysteresis disappears at high enough polymer concentrations where hydrodynamic interactions are fully screened, and the frictional drag coefficient is thus independent of polymer conformation.[23] More recently, ref 24 postulated that the coil−stretch transition and hysteresis can influence the time-dependent decrease in the radius of liquid necks undergoing capillary-driven pinching and the concentration-dependent variation of λ_E.

When the polymer chain conformation changes from coiled to stretched, HI are progressively screened,[15] and the previous simple physical picture describing the magnitude and concentration regimes of λ_E may no longer hold. Indeed, in stretched configurations polymer chains overlap at concentrations $c \ll c^*$.[25] Under strong extensional flow, a stretched single chain behaves like a Rouse chain of tension blobs and retains HI and EV interactions captured by the Zimm model below the length scale of a tension or Pincus blob.[26] In the single chain limit, the size of a tension blob is dependent on the stretching force. The overall drag depends on conformation and change in HI. Thus, after strong extensional flow stretches polymer chains, interchain interactions manifest even for the nominally dilute regime defined via c^* determined using unperturbed coil size.[27,28] The dilute terminology is thus valid only below the stretched overlap concentration c_s^*, where individual chains can fully deform without interacting with other chains.[24,25,29]

Only thermodynamic considerations determine blob size for the "intrinsically" semidilute solutions ($c > c^*$), so defined by ref 30 to emphasize overlap of unperturbed coils. As blob size and number are governed by the degree of stretching, however, interchain interactions in the response to extensional flows as well as λ_E are sensitive to macromolecular strain and extensibility L_E. Extensibility is defined as $L_E = L_c/R_{us}$, the ratio of full stretched or contour length L_c to unperturbed chain size or unstretched length R_{us}, or as $L_E = N_k^{1-\nu}$, a function of the number of Kuhn segments N_k and the Flory exponent ν.

Progress in connecting macromolecular properties to rheological and processing behavior was hampered by longstanding challenges in characterizing the extensional rheology response and the lack of both experimental data and theoretical results for stretched chain hydrodynamics (beyond the single chain limit). References 24 and 30−33 introduced a dripping-onto-substrate (DoS) rheometry protocol as a technique that provides a frugal measurement of elasticity (or λ_E) and η_E. Under extensional flow, polymer chains relax exponentially from elongational stress on a characteristic time scale, λ_E,[13,34] that can be observed experimentally only at concentrations above a minimum concentration c_{min} required to measure the elastic contribution of the polymer.[35] In the dilute regime defined via c^*, λ_E exhibits a power-law dependence $\lambda_E \propto c^m$ that deviates from the predicted linear concentration dependence for the Rouse mode of relaxation in dilute solutions $\lambda = \lambda_{RZ}(1 + k_H[\eta]c)$, where λ_{RZ} is the infinite dilution lifetime and k_H is the Huggins constant,[30,36] due to chain interactions. References 24 and 30 postulated that the dynamics of semidilute polymer solutions described by a Rouse−Zimm chain model could be employed to rationalize the scaling relations of dilute stretched chains in extensional flow. In blob theory,[1,5,37] the concentration dependence of the relaxation time of a Rouse−Zimm chain scales as[30]

$$\lambda \approx \frac{\eta_s b^3}{kT}\left(\frac{N_k b_k{}^3 N_A}{M_w}\right)^m c^m \tag{1}$$

where $m = (2 - 3\nu)/(3\nu - 1)$. Under this framework, refs 24 and 30 related the limiting values of m determined from eq 1 to the EV interactions: the value of 0.31 for a good solvent (for which the Flory exponent $\nu = 0.588$) implies the presence of EV interactions, whereas the value of 1 for a theta solvent ($\nu = 1/2$) implies full screening of EV interactions due to chain stretching.

Most power-law exponents measured in extensional flow experiments, however, fall between the two limits,[35,38] suggesting that quantitative prediction requires understanding of the additional effects that are present due to elongational flow but not considered in blob theory. Previous studies on poly(ethylene oxide) (PEO) in water[31] and glycerol−water mixtures[38] (good solvents) observed a power-law exponent of $m = 0.65$. A study on polystyrene[35] found an exponent of $m = 0.58$ in diethyl phthalate (near good solvent) and $m = 0.89$ in styrene monomer (near theta solvent). Studies on polyacrylamide[39] and partially hydrolyzed polyacrylamide[40] solutions in water, glycerol, and their mixtures found exponents $m = 0.77-0.89$.

Toward this end, refs 24 and 30 connected the concentration dependence of the extensional relaxation time λ_E for $c < c^*$ to polymer macromolecular properties.[24] The elastic responses of poly(ethylene oxide) (PEO) and 2-hydroxyethyl cellulose (HEC) solutions were measured as a function of concentration and compared to predictions in concentration regimes delineated by c_{min} and a stretched overlap concentration c_s^*. The parameter c_s^* was derived from the theory for rod-like polymers in the semidilute regime[2] based on macromolecular parameters. Although both polymers

https://doi.org/10.1021/acs.macromol.3c00097
Macromolecules 2023, 56, 4919−4928

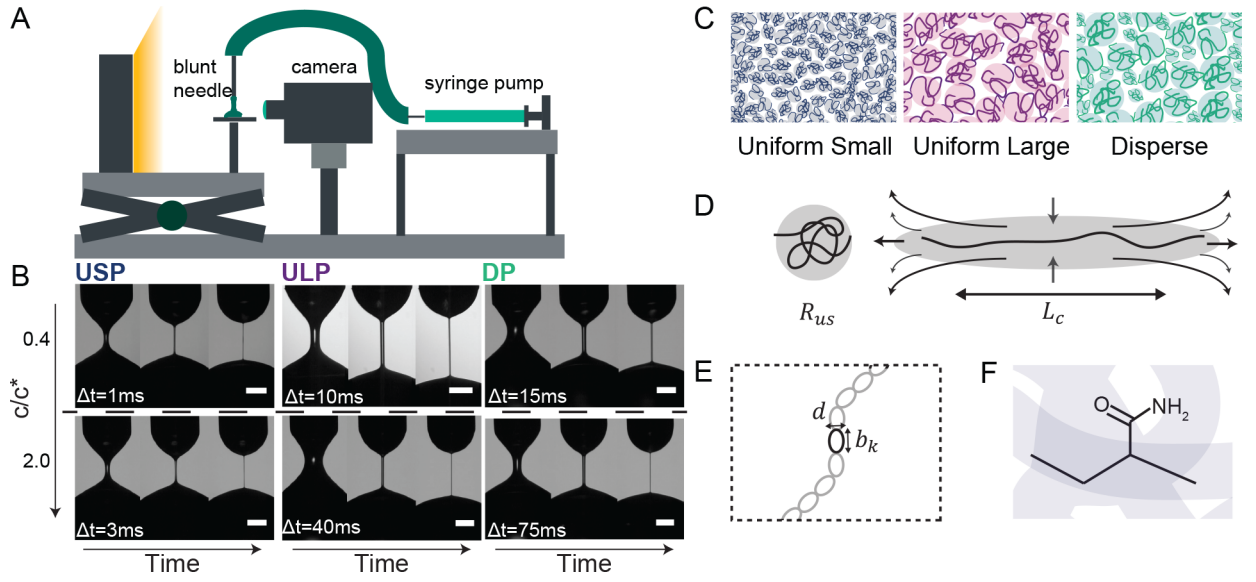

Figure 1. Pinching dynamics of PAM solutions investigated using a dripping-onto-substrate (DoS) protocol. (A) Schematic of the DoS setup used in this study includes high-speed imaging of a polymer solution liquid bridge over time undergoing a capillary-driven instability. (B) Images of pinch-off dynamics of PAM solutions reveal that the breakup time for DP solutions is greater than that for USP and ULP solutions at equal c/c^*. Scale bars are 0.5 mm. (C) Diagrams of varying polymer molecular weight and polydispersity investigated in this study: uniform small polymer (USP), uniform large polymer (ULP), and disperse polymer (DP). (D) Length scales of polymer in quiescent coiled state (unstretched length R_{us}) and stretched state (contour length L_c). (E) Macromolecular properties of polymer defined from their Kuhn segments: Kuhn length b_k and diameter d. (F) Chemical structure of the monomer building block of PAM.

have the same c^*, PEO is more flexible and extensible than HEC based on their estimated contour length L_c, Kuhn length b_k, and unperturbed coil length R_{us} values. For HEC, m_{HEC} = 0.32 at $c^* < c < c_e$ is close to the prediction from blob theory. For PEO, however, m_{PEO} = 0.65 at $c_s^* < c < c^*$ is the geometric mean of the two limits of the blob theory prediction. The values of the exponents suggested that EV interactions govern the extensional response in HEC, whereas chain stretching partially screens the EV interactions in PEO. The differences in exponent were attributed to the extent of screening of EV interactions due to coil−stretch hysteresis of the polymer chains.[24,30] It is incompletely understood, however, how controlling the polymer size distribution may alter the concentration-dependent response by modifying the extent of coil−stretch hysteresis.

Practical applications also require an understanding of the role of the molecular weight distribution on the extensional flow properties. The extensional rheology response is particularly sensitive to L_E, and often highly extensible chains are added to formulations to improve stringiness and spinnability.[41] Recent studies found that the spinnability parameters of disperse polymer solutions are better predicted from an extensibility-averaged molecular weight M_L than weight-averaged M_w or number-averaged molecular weight M_n.[41−44] How the concentration regimes of stretched polymer chains change with dispersity, and whether the prediction from macromolecular parameters is sufficient remains an open question. A fundamental understanding of the different concentration regimes of extensional relaxation time and their dependence on the polymer molecular weight distribution will enable better control over the processability of materials.[45]

In this contribution, we use a modified DoS rheometry protocol (Figure 1A,B) based on refs 24 and 30−33 to measure λ_E of unentangled polyacrylamide (PAM) solutions, and we elucidate the influence of molecular weight and dispersity on the concentration-dependent variation in λ_E. Polyacrylamide is a linear water-soluble polymer often used in turbulent drag reduction,[46] as a viscosifier for enhanced oil recovery,[47] and for biocompatible fiber materials.[48,49] We find that concentration regimes of extensional relaxation time λ_E for PAM depend on the polymer physical properties derived from intrinsic viscosity measurements and the molecular weight. The extensional response of PAM solutions is better predicted with M_w, especially for a highly disperse solution, highlighting the importance of long polymer chains. The extensional behavior is consistent with other polymer systems (PEO and HEC),[24] implying that concentration-dependent response can be controlled through polymer size and dispersity.

MATERIALS AND METHODS

We prepared three series of solutions of PAM with various molecular weights and dispersities: M_w = 194 kDa, $Đ$ = 1.24, Polymer Source, Uniform Small Polymer (USP); M_w = 1.00 MDa, $Đ$ = 1.25, Polymer Source, Uniform Large Polymer (ULP); and M_w = 1.97 MDa, $Đ$ = 21, Sigma-Aldrich, Disperse Polymer (DP) (Figure 1C). The differences in polymer size will consequently lead to variation in the unstretched length or coil length R_{us} and stretched length or contour length L_c of the polymer (Figure 1D). Additional length scales, such as the Kuhn length b_k and diameter d (Figure 1E) as well as the monomer length l_0, bond length l, and monomer molecular weight M_0 (Figure 1F), are assumed to be constant across the three PAM. Polymer powder was dissolved into 80% w/w glycerol−water to make stock solutions, which were mixed at low speed (~7 rpm) on a roller to prevent chain scission[50−52] for at least 1 week to ensure homogenization.

The shear viscosity η as a function of shear rate $\dot{\gamma}$ was measured with a DHR-2 rheometer (TA Instruments, New Castle, DE) with minimum torque 2 μN·m on a 40 mm diameter cone-and-plate hard-anodized aluminum geometry. Polymer solutions were treated with a consistent preshear protocol[53] before every flow sweep (Supporting Information). We used a DoS protocol (Figure 1A,B) modified from that in refs 31 and 32 (Supporting Information) to characterize the

https://doi.org/10.1021/acs.macromol.3c00097
Macromolecules 2023, 56, 4919−4928

extensional rheology response due to the low viscosity and low elasticity of most of our PAM solutions.

RESULTS AND DISCUSSION

The steady shear viscosity of the three solutions (USP, ULP, and DP) is nearly independent of the shear rate in the dilute regime ($c/c^* = 0.4$, estimated from $c^* \approx 1/[\eta]$) (Figure 2A).

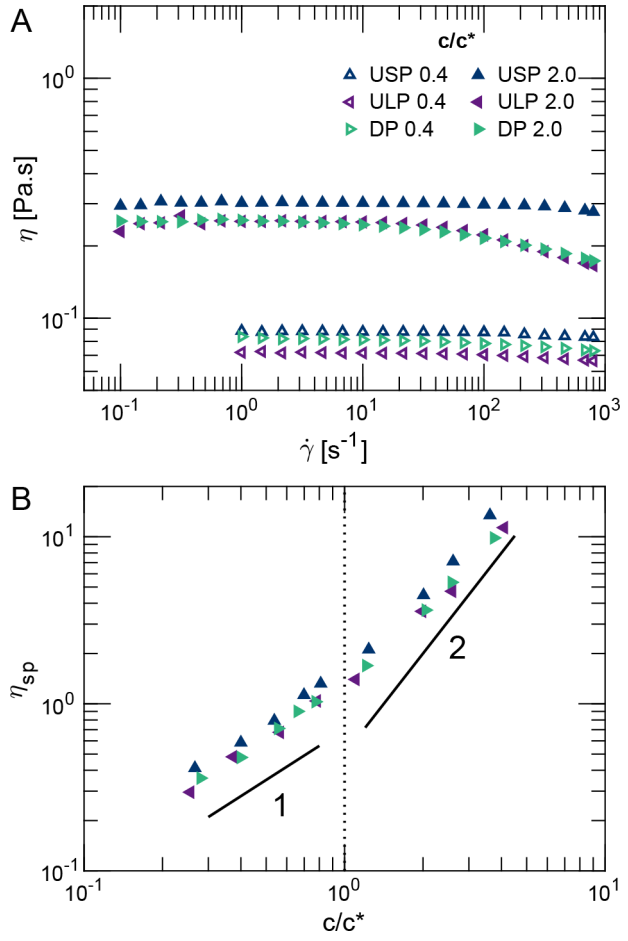

Figure 2. Shear rheology of PAM solutions in 80% w/w glycerol–water with 1.5 mM NaCl. (A) Flow curves of representative USP, ULP, and DP polyacrylamide solutions at matched c/c^* in the dilute and semidilute unentangled regimes. (B) Specific viscosity η_{sp} of PAM solutions as a function of normalized concentration c/c^*. Data from all three solutions were collapsed onto a master curve, as expected for neutral polymer rheology.

ULP and DP solutions exhibit shear-thinning behavior in the semidilute regime ($c/c^* = 2.0$), whereas the USP solution exhibits a Newtonian-like response. The specific viscosity $\eta_{sp} = (\eta_0 - \eta_s)/\eta_s$, where η_0 is the viscosity measured at the lowest accessible shear rate and η_s is the solvent viscosity, collapses onto a master curve as a function of the normalized concentration c/c^* (Figure 2B). The linear concentration dependence in the dilute regime $\eta_{sp} \sim (c/c^*)^1$ and quadratic scaling of $\eta_{sp} \sim (c/c^*)^2$ in the semidilute unentangled regime are consistent with scaling theory predictions for neutral polymers.[5] The scaling behavior and master curve are similar to those obtained in an earlier study of aqueous PAM solutions.[54]

The physical properties of PAM solutions were calculated from the molecular weight and the intrinsic viscosity $[\eta]$ (Supporting Information). The excluded volume exponent for PAM in 80% w/w glycerol–water, estimated from $[\eta]$ via the Mark–Houwink equation (Supporting Information), is $\nu \sim 0.6$, suggesting that 80% w/w glycerol–water is a good solvent for PAM. The viscosity-averaged molecular weight M_v of DP calculated from $[\eta]$ is 570 kDa, consistent considering the large dispersity of the sample.

Using a modified DoS protocol (Figure 1A and Supporting Information), we determined the time-dependent evolution of the neck radius for the polymer solutions. Images of the filament breakup for USP, ULP, and DP solutions of equal c/c^* reveal that the DP solution exhibits the longest breakup time (Figure 1B). We extracted the time-dependent filament radius from the images. High-viscosity Newtonian fluids such as the background solvent exhibit a viscocapillary (VC) response,[13,55,56] for which

$$\frac{R(t)}{R_0} = \frac{2X_{vc} - 1}{6}\left(\frac{\sigma}{\eta_0 R_0}\right)(t_f - t) \tag{2}$$

where σ is the surface tension, η_0 is the zero-shear viscosity, R_0 is the nozzle radius, X_{vc} is a numerical prefactor[57] that varies across experiments and is of $O(1)$,[58] and t_f is the total filament timespan.

The dominance of viscous forces during pinch-off is typically predicted from the Ohnesorge number $\mathrm{Oh} = \eta_0/(\rho\sigma R_0)^{1/2}$, which compares the magnitude of the viscous forces to those of the inertial and surface tension forces. When $\mathrm{Oh} > 1$, the time evolution of the radius follows VC scaling. By contrast, Newtonian fluids with $\mathrm{Oh} < 1$ instead exhibit an inertio-capillary (IC) response[56,59,60] for which

$$\frac{R(t)}{R_0} = X_{ic}\left(\frac{\sigma}{\rho R_0^3}\right)(t_f - t)^{2/3} \tag{3}$$

where ρ is fluid density and X_{ic} is a $O(1)$ numerical prefactor with various experimentally determined values.[58] Both VC and IC equations are adapted from ref 56.

We use a generalized power-law (PL) relationship[30,56] to estimate the scaling exponent of our samples without prior assumption on their scaling response, given as

$$\frac{R(t)}{R_0} = Y(t_f - t)^{n_e} \tag{4}$$

where n_e is the power-law exponent and Y is a constant that represents the material intrinsic properties. From this fitting, we observe VC scaling at the later part of the pinch-off process for our glycerol–water solvent (Figure 3A) despite having Oh = 0.17 because the filament radius approaches the Ohnesorge unit length $l_{Oh} = \eta^2/(\sigma\rho) = 38\ \mu m$.[58]

By contrast, the pinching dynamics of PAM solutions display an initial regime that scales with a power-law (PL) exponent followed by a second regime that exhibits an elastocapillary (EC) response, in which the filament radius decays exponentially with time according to[13,61]

$$\frac{R(t)}{R_0} = \left(\frac{G_E R_0}{2\sigma}\right)^{1/3} \exp[-(t - t_c)/3\lambda_E] \tag{5}$$

where G_E is the elastic modulus and t_c is the transition time from PL to EC response. The prefactor corresponds to the

https://doi.org/10.1021/acs.macromol.3c00097
Macromolecules 2023, 56, 4919–4928

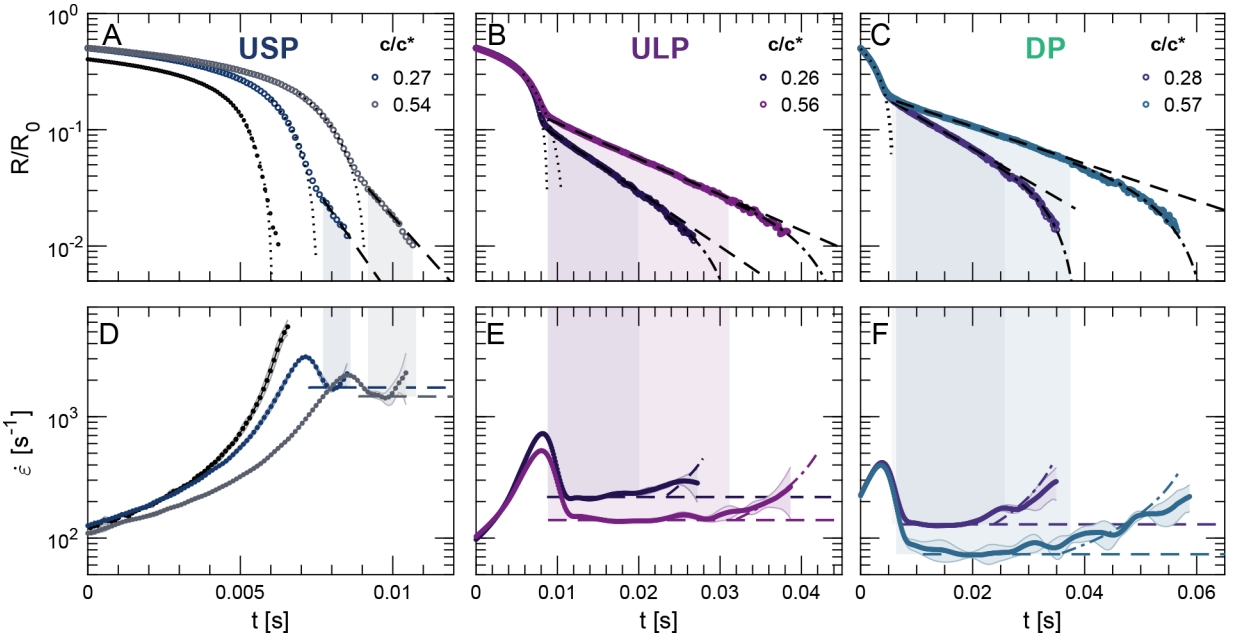

Figure 3. Radius evolution of (A) USP, (B) ULP, and (C) DP polyacrylamide solutions in 80% w/w glycerol−water as a function of time. Dotted lines in (A) indicate viscocapillary (VC) scaling and in (B) and (C) indicate power-law (PL) scaling. Dashed lines indicate elastocapillary (EC) scaling, and the shaded area indicates the EC regime. Dash-dotted lines indicate terminal visco-elastocapillary (TVEC) scaling. The derivative of the radius evolution $\dot{\varepsilon} = (-2/R)(dR/dt)$ for (D) USP exhibits a peak followed by a plateau or slight decrease; for (E) ULP and (F) DP, $\dot{\varepsilon}$ exhibits a sharp decrease and a constant strain rate upon reaching the EC regime and a subsequent increase upon entering the TVEC regime prior to pinch-off. Errors in strain rate are derived from averaging multiple replicates at matched peak $\dot{\varepsilon}$. For polymer solutions, we define $t = 0$ as the time at which $R/R_0 = 0.50$; for the solvent (black circle), we define $t = 0$ as the time at which $R/R_0 = 0.40$.

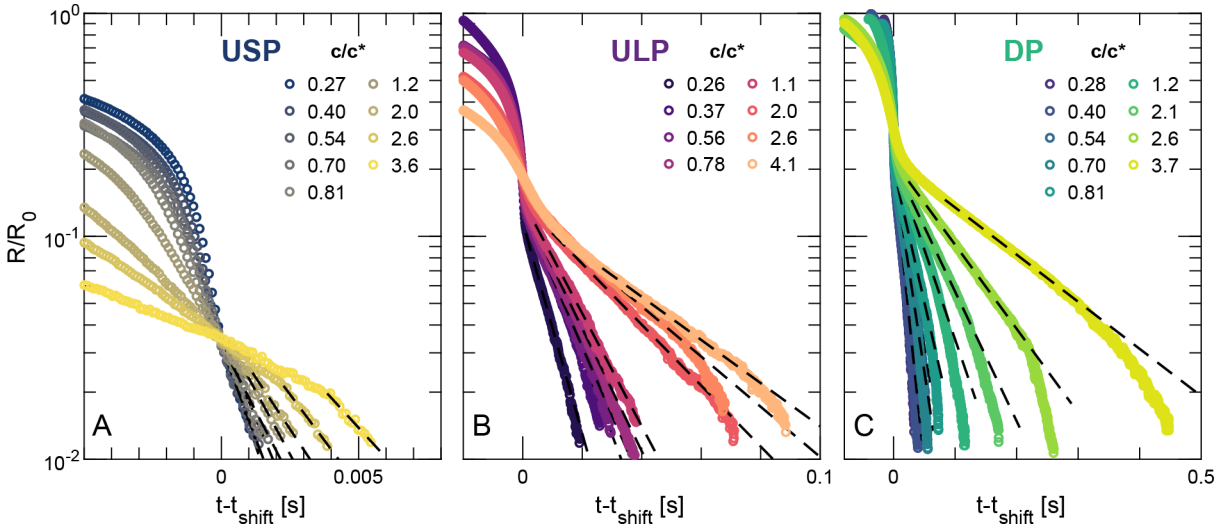

Figure 4. Pinching dynamics of USP, ULP, and DP polyacrylamide solutions in 80% w/w glycerol−water with 1.5 mM NaCl. Neck radius evolution shifted by the t_{shift} value displays a concentration-dependent EC response. We define t_{shift} as the time at which $R/R_0 = 0.03$ for USP, $R/R_0 = 0.18$ for ULP, and $R/R_0 = 0.30$ for DP. Dashed lines indicate EC fitting (eq 5).

critical radius $R_c \approx R_0(G_E R_0/2\sigma)^{1/3}$ of the transition. The distinct radius evolution profile of the PL and EC responses for PAM solution is illustrated in Figure 3A−C, where the radius evolution transitions from a linear to an exponential scaling for all PAM solutions.

At $t = t_c$, ULP and DP (Figure 3B,C) exhibit a much sharper transition to the EC than does USP (Figure 3A). The magnitude of change in radius evolution scaling is quantified from the derivative of R/R_0 with time, from which the extensional strain rate $\dot{\varepsilon} = (-2/R)(dR/dt)$ is determined. The strain rate magnitude of USP attains a peak at the transition to the EC regime and subsequently plateaus or slightly decreases as pinch-off is reached (Figure 3D). By contrast, $\dot{\varepsilon}$ values for ULP and DP also exhibit similar peaks but thereafter decrease abruptly to a constant value throughout the EC regime (Figure 3E,F). Reference 24 suggests that this sharp decrease is a signature of the coil−stretch transition. We also observe another qualitative discrepancy on long time scales, where the terminal visco-elastocapillary (TVEC) regime[13,33] is absent in USP but prominent in ULP and DP. On long time scales, the scaling regime deviates from

https://doi.org/10.1021/acs.macromol.3c00097
Macromolecules 2023, 56, 4919−4928

Table 1. Rheological Parameters Measured for Each Polymer at Similar c/c^* Values from Shear and Extensional Measurements[a]

c (g/L)	η_0 (Pa·s)	Oh	R_c (μm)	t_c (ms)	t_f (ms)	λ_E (ms)
			USP			
3.2	0.079	0.25	45 ± 5	7.5 ± 0.1	8.5 ± 0.06	0.39 ± 0.004
6.5	0.10	0.31	56 ± 4	8.3 ± 0.5	9.7 ± 0.6	0.46 ± 0.03
9.9	0.13	0.40	49 ± 7	9.3 ± 0.3	11 ± 0.2	0.53 ± 0.05
24	0.30	0.95	32 ± 6	31 ± 2	32 ± 1	0.69 ± 0.07
44	0.80	2.5	36 ± 6	71 ± 2	74 ± 1	1.1 ± 0.1
			ULP			
0.82	0.072	0.22	145 ± 3	8.4 ± 0.3	25 ± 0.5	3.1 ± 0.06
1.8	0.093	0.29	167 ± 3	9.0 ± 0.2	37 ± 0.6	4.7 ± 0.04
2.5	0.11	0.35	168 ± 7	9.8 ± 0.6	42 ± 0.6	5.3 ± 0.1
6.4	0.26	0.79	180 ± 10	21 ± 1	87 ± 1	11 ± 0.1
13	0.69	2.1	160 ± 10	52 ± 2	130 ± 2	15 ± 0.7
			DP			
1.4	0.076	0.24	250 ± 2	4.9 ± 0.1	36 ± 0.9	5.2 ± 0.07
2.8	0.095	0.30	230 ± 30	6 ± 2	56 ± 2	8.9 ± 1
3.9	0.11	0.35	262 ± 6	5.9 ± 0.2	77 ± 2	12 ± 0.2
10	0.26	0.81	291 ± 9	20 ± 1	190 ± 4	25 ± 0.3
19	0.60	1.9	299 ± 7	33 ± 1	460 ± 8	68 ± 2

[a]Background solvent viscosity η_0 of 80% w/w glycerol−water is measured at 0.056 Pa·s.

exponential and is instead linear ($R/R_0 \sim (t_f - t)$) due to the finite extensibility effect. The slope from the TVEC scaling follows $\sigma/2R_0\eta_{E,\infty}$, and we confirmed that the terminal steady-state extensional viscosity $\eta_{E,\infty}$ from the TVEC fitting matches the η_E calculated from the numerical derivation ($\eta_E = -\sigma/2\ dR/dt$). The differences in the EC and TVEC regime time spans between ULP and DP may arise from the system polydispersity. The mixtures of short and long chains in DP potentially allow the bulk solution to experience a finite extensibility effect at an earlier stage compared to that of a solution of lower dispersity.

To illustrate the concentration-dependent elastic response, we shift the radius evolution with t_{shift}. All three PAM solutions exhibit an elastic response that follows the EC scaling (Figure 4) in the dilute regime for concentrations greater than c_s^*. USP solutions exhibit a weaker EC response (i.e., a weaker exponential decay) than do ULP or DP solutions. Very dilute ULP and DP solutions with $c < c_s^*$ exhibit a similar short EC regime and transition close to pinch-off. The difference in the qualitative shape of the time evolution of the filament radius for USP versus ULP and DP may arise from the weaker elastic contribution of USP in comparison with the larger polymers.

By fitting the exponential decay with eq 5 (dashed lines), we quantify the elastic response via λ_E. To compare the different elasticity measures for dilute solutions, we calculate the Zimm relaxation time $\lambda_z = [\eta]\eta_s M_w/U_{\eta\tau}RT$, where the prefactor $U_{\eta\tau} = \sum_{i=1}^{\infty} \frac{1}{i^{3\nu}}$ is the universal ratio.[6,35] The estimated values of λ_z for USP, ULP and DP are respectively, 0.19, 3.8, and 4.8 ms. The λ_E values for USP never fall below the predicted λ_z at very dilute concentrations, whereas λ_E for ULP and DP continues to decrease with concentration and can be up to an order of magnitude smaller than λ_z. These results are consistent with measurements for polystyrene in styrene oligomer[35] and for a similar system of PAM in glycerol−water mixtures.[40] The comparison emphasizes the distinct concentration-dependent time scale that governs polymer relaxation under stretching flow.

Representative parameters for both shear and extensional measurement are tabulated in Table 1, where the background solvent of 80% w/w glycerol−water is measured to have Oh = 0.17. The Ohnesorge number of the solutions transitions from $O(0.1)$ to $O(1)$ with increasing polymer concentration. This result indicates a transition from inertial- to viscous-dominated dynamics, which may contribute to the differences in the Newtonian regime prior to the elastic response in Figure 4. Polymer size strongly affects R_c, which results in scaling differences among the polymers. R_c is smaller than l_{Oh} for all USP solutions but larger for ULP and DP solutions until $c > c^*$. The radius evolution of USP follows the VC scaling, whereas the radii of ULP and DP scale as a power-law with an exponent of $n_e \sim 0.7-1$.

Extensional responses across PAM solutions differ significantly by polymer size, indicating that c^* is not a good scaling parameter to understand molecular weight contributions. Polymer size strongly affects both the practical processing time scale t_f and the characteristic time scale of elasticity λ_E probed in DoS measurements. Large polymers can increase the time scale significantly at a smaller mass concentration, and both t_f and λ_E from DP solutions appear to be dominated by the larger polymers in the distributions. Overall, t_f is dominated by the EC regime, suggesting that polymer elasticity has stronger contributions, and further analysis of λ_E may elucidate the physical picture of the behavior.

We apply the framework used in ref 24 to understand the role of polymer size by calculating macromolecular parameters as criteria for coil−stretch hysteresis. To determine whether our PAM solutions exhibit coil−stretch hysteresis, we compare the ratio of the drag coefficient of stretched $\varsigma_s = (2\pi\eta_s L_c)/\ln(L_c/d)$ and coiled $\varsigma_c = (3/8)(6\pi^3)^{1/2}\eta_s R_{us}$ chains,[3] which are a function of the different polymer length scales (Figure 1D−F), to the criterion $\varsigma_s/\varsigma_c > 4.5$.[20]

Here, we estimate contour length $L_{c,w} = \sin(\theta/2)N_w l_0$ from the degree of polymerization $N_w = M_w/M_0$.[3] We consider both linear $\theta = 180°$ and *all-trans* $\theta = 109.5°$ configurations. The Kuhn segment diameter d is calculated from the packing length

https://doi.org/10.1021/acs.macromol.3c00097
Macromolecules 2023, 56, 4919−4928

Table 2. Macromolecular Parameters of Polyacrylamide Characterized from Supplier Information, Intrinsic Viscosity Measurements, and Estimations from Molecular Properties[a]

Parameters		USP	ULP	DP
$[\eta]$ (mL mg^{-1})	intrinsic viscosity	0.082	0.31	0.54,[b] 0.20[c]
λ_z (ms)	Zimm relaxation time	0.19	3.8	4.8
c^* (mg mL^{-1})	overlap concentration	12	3.2	5.1,[b] 1.8[c]
R_g (nm)	radius of gyration	19	50	36,[b] 75[c]
R_{us} (nm)	unstretched polymer length	47	122	184
N_w	degree of polymerization	2732	14085	27746
L_c (nm)	contour length	687−842	3543−4338	6979−8546
N_k	number of Kuhn segments	643−787	3315−4059	6530−7996
L_E^2	finite extensibility parameter	218−327	837−1255	1443−2164
ς_s/ς_c	drag coefficient ratio	2.5−3.0	4.0−4.8	4.9−5.9
c_{min}/c^* ($\times 10^3$)	minimum concentration	8.6−13	2.2−3.4	1.3−2.0
c_s/c^* ($\times 10^2$)	overlap stretched concentration	20−30	14−21	12−18

[a]The range of values arises from two bond angles (linear $\theta = 180°$ and *all-trans* $\theta = 109.5°$). Basic shared parameters are $M_0 = 71$ g mol^{-1}, $b_k = 1.1-1.3$ nm, and $d = 0.6$ nm. [b]Experimental measurement. [c]Estimated from $[\eta] = kM_v^a$.

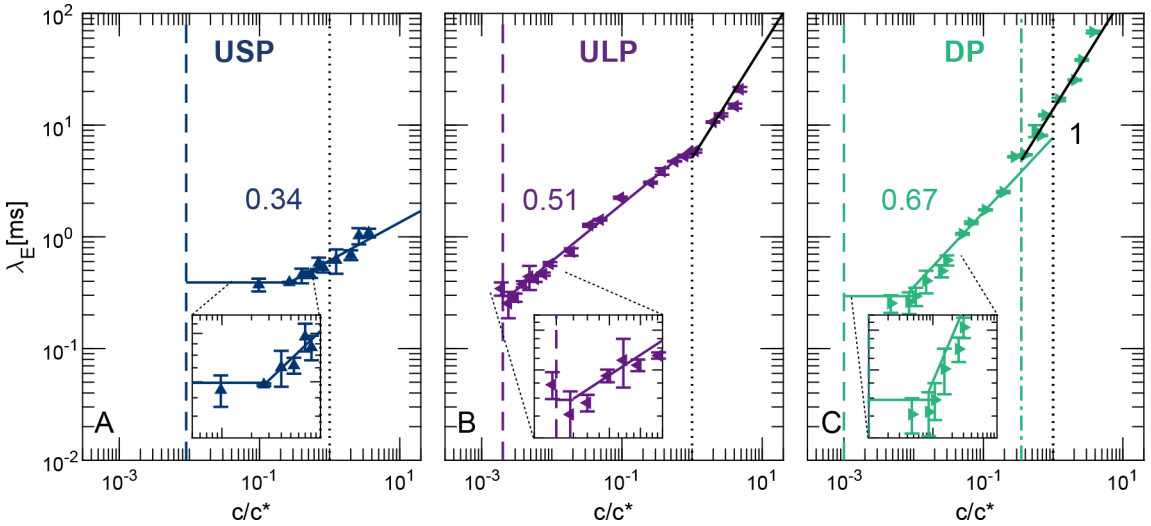

Figure 5. Extensional relaxation time λ_E for polyacrylamide solutions as a function of normalized concentration c/c^*. The dashed vertical lines indicate the predicted minimum concentration c_{min} needed to observe the elastocapillary response for each polymer. The black dotted vertical lines indicate the transition from dilute to semidilute regime. For DP solutions, the vertical dashed dotted line indicates the overlap concentration c^* derived from the Mark−Houwink equation and M_w. Power-law exponents extracted from the fitting are 0.34 ± 0.06 for USP, 0.51 ± 0.02 for ULP, and 0.67 ± 0.07 for DP. Error bars are determined from the standard deviation of multiple replicates. Inset: transition to the concentration-independent regime of λ_E at low concentration limit.

$p = (\pi/4)d_k^2/b_k \approx d^2/b_k$ and actual diameter $d_k = 4M_0/\sin(\theta/2)j\pi lN_{av}\rho$, where j is the number of backbone bonds in the monomer, l is the bond length, N_{av} is Avogadro's number, and ρ is the polymer density.[3] The polymer length scales, the radius of gyration[62] $R_g = M_w/(4/3)\pi N_{av}c^*$ with $c^* = 1/[\eta]$, and the unstretched polymer length[3] $R_{us} = R_g\sqrt{6}$ are determined from shear rheology under near-quiescent conditions. For DP, we use the value of $[\eta]$ estimated from M_w to calculate the relevant parameters. We calculate the flexibility, represented by the number of Kuhn segments[3,24] $N_k = L_{c,w}/b_k$, the extensibility[6,24] $L_E^2 = (L_{c,w}/R_{us})^2$, and the segmental dissymmetry[24] $S_d = (b_k/d)^2$. Finally, we predict the delineation of concentrations using $c_{min}/c^* = 3/2L_E^2U_{\eta\tau}$[35] and $c_s^*/c^* = (4/3)\pi R_g^3/dL_{c,w}^2$.[2] All relevant parameters are listed in Table 2.

For low c/c^*, λ_E is independent of concentration (Figure 5), as expected for $c_{min} < c < c_s^*$. We determine the concentration-independent regime as the regime in which the relaxation time is approximately within to the standard deviation. The prediction of the transition from the polymer macromolecular parameters $c_s^*/c^* \approx N_k(b_k/d)/L_E^3$, where N_k is the number of Kuhn segments, d is the hydrodynamic bead diameter, and L_E^2 is the extensibility,[24] is within an order of magnitude of our experimental results. The consistency between the experimentally measured and theoretically predicted values of c_s^* supports the use of macromolecular parameters to delineate the concentration regimes.

Using the linear configuration, we estimate for USP $\varsigma_s/\varsigma_c < 4.5$ and for ULP and DP $\varsigma_s/\varsigma_c > 4.5$, indicating that coil−stretch hysteresis occurs in ULP and DP solutions but not in USP solutions.[20,24] The experimentally measured scaling exponents of λ_E with concentration are consistent with the calculated ς_s/ς_c: $m_{USP} = 0.34 \pm 0.06$, close to 0.31 predicted for hydrodynamic interactions, and $m_{ULP} = 0.51 \pm 0.02$ and $m_{DP} = 0.67 \pm 0.07$, close to the geometric mean of the two limiting exponents and indicative of EV screening. The increase in the drag coefficient ratio between ULP and DP is due to the M_w of DP, which is almost twice that of ULP, and may also

https://doi.org/10.1021/acs.macromol.3c00097
Macromolecules 2023, 56, 4919−4928

contribute to the degree of partial EV screening, as $m_{DP} > m_{ULP}$.

At higher concentrations, the scaling exponent transitions to unity for ULP and DP solutions. This transition occurs at c^* for ULP solutions, as expected for full screening of the EV interactions. For DP solutions, however, the transition to linear scaling occurs at $c/c^* \sim 0.28$. This value is close to the overlap concentration of DP derived from Mark−Houwink parameters from USP and ULP solutions using the M_w of DP, $c/c^* \sim 0.35$. This result suggests that the transition to the semidilute regime under extensional flow may be better described by overlap concentration c^* that is representative of M_w instead of M_v obtained from shear rheology.

An earlier study of the capillary breakup of PAM with M_w = 5−6 MDa in glycerol−water mixtures[39] found the power-law exponent exhibited a stronger concentration dependence (m = 0.82 ± 0.04) over a range of concentrations spanning c^*. This value is comparable to the exponent obtained by fitting our DP data from $c_s^* < c < c^*$ ($m_{DP,span}$ = 0.85 ± 0.09). Thus, whereas the higher exponent in their study may be due to the increase in EV screening as some data points were in the $c > c^*$ regime, our results suggest that this stronger concentration dependence may arise from a shift of effective c^* due to high dispersity. The importance of high molecular weight polymers in the extensional rheology of disperse polymer solutions is consistent with earlier observations of the spinnability of disperse polymer solutions.[41,42]

From the scaling relationship, we also examine the monomer relaxation time $\lambda_0 \approx \eta_s b^3/kT$, which can be substituted into eq 1 as a way to quantitatively predict the concentration dependence of the relaxation time across molecular weight.[30] When the segment length is approximated as $b_k \approx 1.1$ nm, the predicted λ_0 is 18 ns. We find that when λ_0 is extracted from the slope of λ_E scaling, we obtain 0.25, 0.33, and 0.16 ns from USP, ULP, and DP, respectively, differing from the value predicted from the segment length. The λ_0 values extracted from λ_E, however, could predict Zimm relaxation time $\lambda_z \approx \lambda_0 N^{3\nu}$ within an order of magnitude, as also found in the PEO in water system.[30] The predicted λ_z is close to the value corresponding to the weight-averaged estimated $[\eta]$, which supports our conclusion that the weight-averaged parameter better predicts the extensional response of the polymer solutions.

CONCLUSION

Our study connects the macromolecular parameters to the concentration-dependent extensional response of polyacrylamide (PAM) solutions under extensional flow and intriguingly suggests that we can vary polymer size and dispersity as an option to tailor the material response. The polymer size qualitatively controls the pinch-off dynamics, where larger polymers (ULP and DP) introduce a distinct transition to the elastocapillary (EC) regime that is characterized by the discrete overshoot in strain rate. These differences are not observed in the shear rheology characterization when compared at similar normalized concentration c/c^* in the dilute regime $c/c^* < 1$. As polymer concentration increases, the concentration-dependent response in EC regime exhibits a power-law scaling that depends on polymer size. The scaling exponents characterizing the concentration dependence of λ_E increase with ς_s/ς_o (i.e., $m_{USP} < m_{ULP} < m_{DP}$), consistent with previous studies.[24,30]

The full screening of EV interactions also depends on the overlap concentration c^* determined from M_w, leading to a transition to linear scaling at lower c values in highly disperse solutions. This result indicates that the larger polymers in a polydisperse mixture contribute more significantly to the solution dynamics.

Future studies in more complicated systems such as polyelectrolytes are expected to provide additional insight into factors controlling concentration-dependent material response for applications in polymer processing and advanced manufacturing.

ASSOCIATED CONTENT

Supporting Information

The Supporting Information is available free of charge at https://pubs.acs.org/doi/10.1021/acs.macromol.3c00097.

Protocols for shear rheology and DoS; additional calculation of the macromolecular parameters of PAM, summarized in Table 2; gel permeation chromatography traces of the polymers; captions for Movies S1−S3 (PDF)

Movie S1 (MP4)

Movie S2 (MP4)

Movie S3 (MP4)

AUTHOR INFORMATION

Corresponding Authors

Vivek Sharma − *Department of Chemical Engineering, University of Illinois Chicago, Chicago, Illinois 60607, United States;* orcid.org/0000-0003-1152-1285; Email: viveks@uic.edu

Jacinta C. Conrad − *Department of Chemical and Biomolecular Engineering, University of Houston, Houston, Texas 77204, United States;* orcid.org/0000-0001-6084-4772; Email: jcconrad@uh.edu

Authors

Diego D. Soetrisno − *Department of Chemical and Biomolecular Engineering, University of Houston, Houston, Texas 77204, United States*

Carina D. V. Martínez Narváez − *Department of Chemical Engineering, University of Illinois Chicago, Chicago, Illinois 60607, United States;* orcid.org/0000-0002-2356-7208

Complete contact information is available at: https://pubs.acs.org/10.1021/acs.macromol.3c00097

Notes

The authors declare no competing financial interest.

ACKNOWLEDGMENTS

The authors thank Megan Robertson for access to the DHR-2 rheometer, Alamgir Karim for access to the KronTech high-speed camera, Gerald Blosser for machining of DoS setup, and Christopher Macosko for constructive discussions. J.C.C. acknowledges funding from the National Science Foundation (CBET-1803728) and the Welch Foundation (E-1869).

REFERENCES

(1) de Gennes, P.-G. *Scaling Concepts in Polymer Physics*; Cornell University Press: Ithaca, NY, 1979.

(2) Doi, M.; Edwards, S. F. *The Theory of Polymer Dynamics*; Oxford University Press: New York, 1986.

(3) Larson, R. G. *The Structure and Rheology of Complex Fluids*; Oxford University Press: New York, 1999.
(4) Macosko, C. W. *Rheology: Principles, Measurements, and Applications*; VCH: New York, 1994.
(5) Rubinstein, M.; Colby, R. H. *Polymer Physics*; Oxford University Press: New York, 2003.
(6) Larson, R. G. The rheology of dilute solutions of flexible polymers: Progress and problems. *J. Rheol.* **2005**, *49*, 1−70.
(7) Mishra, R.; Militky, J.; Venkataraman, M. In *Nanotechnology in Textiles*; Mishra, R., Militky, J., Eds.; The Textile Institute Book Series; Woodhead Publishing: Duxford, 2019; pp 35−161.
(8) Jiang, Z.; Diggle, B.; Tan, M. L.; Viktorova, J.; Bennett, C. W.; Connal, L. A. Extrusion 3D Printing of Polymeric Materials with Advanced Properties. *Adv. Sci.* **2020**, *7*, 2001379.
(9) Prakash, J. R. Universal dynamics of dilute and semidilute solutions of flexible linear polymers. *Curr. Opin. Colloid Interface Sci.* **2019**, *43*, 63−79.
(10) Matsumiya, Y.; Watanabe, H. Non-universal features in uniaxially extensional rheology of linear polymer melts and concentrated solutions: A review. *Prog. Polym. Sci.* **2021**, *112*, 101325.
(11) Petrie, C. J. S. One hundred years of extensional flow. *J. Non-Newton. Fluid Mech.* **2006**, *137*, 1−14.
(12) Dinic, J.; Martínez Narváez, C. D. V.; Sharma, V. *Macromolecular Engineering*; John Wiley & Sons, Ltd: Chichester, 2022; pp 1−36.
(13) McKinley, G. H. Visco-elasto-capillary thinning and break-up of complex fluids. *Rheol. Rev.* **2005**, 1−48.
(14) Schroeder, C. M. Single polymer dynamics for molecular rheology. *J. Rheol.* **2018**, *62*, 371−403.
(15) de Gennes, P.-G. Coil-stretch transition of dilute flexible polymers under ultrahigh velocity gradients. *J. Chem. Phys.* **1974**, *60*, 5030−5042.
(16) Tanner, R. I. Stresses in Dilute Solutions of Bead-Nonlinear-Spring Macromolecules. III. Friction Coefficient Varying with Dumbbell Extension. *Trans. Soc. of Rheol.* **1975**, *19*, 557−582.
(17) Hinch, E. J. Mechanical models of dilute polymer solutions in strong flows. *Phys. Fluids* **1977**, *20*, S22−S30.
(18) Schroeder, C. M.; Babcock, H. P.; Shaqfeh, E. S. G.; Chu, S. Observation of polymer conformation hysteresis in extensional flow. *Science* **2003**, *301*, 1515−1519.
(19) Schroeder, C. M.; Shaqfeh, E. S.; Chu, S. Effect of hydrodynamic interactions on DNA dynamics in extensional flow: Simulation and single molecule experiment. *Macromolecules* **2004**, *37*, 9242−9256.
(20) Hsieh, C.-C.; Larson, R. G. Prediction of coil-stretch hysteresis for dilute polystyrene molecules in extensional flow. *J. Rheol.* **2005**, *49*, 1081−1089.
(21) Hsieh, C.-C.; Li, L.; Larson, R. G. Modeling hydrodynamic interaction in Brownian dynamics: simulations of extensional flows of dilute solutions of DNA and polystyrene. *J. Non-Newton. Fluid Mech.* **2003**, *113*, 147−191.
(22) Hsieh, C.-C.; Larson, R. G. Modeling hydrodynamic interaction in Brownian dynamics: Simulations of extensional and shear flows of dilute solutions of high molecular weight polystyrene. *J. Rheol.* **2004**, *48*, 995−1021.
(23) Prabhakar, R. Enhancement of coil-stretch hysteresis by self-concentration in polymer solutions. arXiv (Soft Condensed Matter), January 31, 2013; 1209.0163, Ver. 2. https://arxiv.org/abs/1209.0163 (accessed 2023-04-04).
(24) Dinic, J.; Sharma, V. Flexibility, Extensibility, and Ratio of Kuhn Length to Packing Length Govern the Pinching Dynamics, Coil-Stretch Transition, and Rheology of Polymer Solutions. *Macromolecules* **2020**, *53*, 4821−4835.
(25) Dunlap, P. N.; Leal, L. G. Dilute polystyrene solutions in extensional flows: Birefringence and flow modification. *J. Non-Newton. Fluid Mech.* **1987**, *23*, 5−48.
(26) Pincus, P. Excluded volume effects and stretched polymer chains. *Macromolecules* **1976**, *9*, 386−388.
(27) Prabhakar, R.; Gadkari, S.; Gopesh, T.; Shaw, M. J. Influence of stretching induced self-concentration and self-dilution on coil-stretch hysteresis and capillary thinning of unentangled polymer solutions. *J. Rheol.* **2016**, *60*, 345−366.
(28) Prabhakar, R.; Sasmal, C.; Nguyen, D. A.; Sridhar, T.; Prakash, J. R. Effect of stretching-induced changes in hydrodynamic screening on coil-stretch hysteresis of unentangled polymer solutions. *Phys. Rev. Fluid* **2017**, *2*, 011301.
(29) Harrison, G. M.; Remmelgas, J.; Leal, L. G. The dynamics of ultradilute polymer solutions in transient flow: Comparison of dumbbell-based theory and experiment. *J. Rheol.* **1998**, *42*, 1039−1058.
(30) Dinic, J.; Biagioli, M.; Sharma, V. Pinch-off dynamics and extensional relaxation times of intrinsically semi-dilute polymer solutions characterized by dripping-onto-substrate rheometry. *J. Polym. Sci. B Polym. Phys.* **2017**, *55*, 1692−1704.
(31) Dinic, J.; Zhang, Y.; Jimenez, L. N.; Sharma, V. Extensional relaxation times of dilute, aqueous polymer solutions. *ACS Macro Lett.* **2015**, *4*, 804−808.
(32) Dinic, J.; Jimenez, L. N.; Sharma, V. Pinch-off dynamics and dripping-onto-substrate (DoS) rheometry of complex fluids. *Lab Chip* **2017**, *17*, 460−473.
(33) Dinic, J.; Sharma, V. Macromolecular relaxation, strain, and extensibility determine elastocapillary thinning and extensional viscosity of polymer solutions. *Proc. Natl. Acad. Sci. U. S. A.* **2019**, *116*, 8766−8774.
(34) Bousfield, D. W.; Keunings, R.; Marrucci, G.; Denn, M. M. Nonlinear analysis of the surface tension driven breakup of viscoelastic filaments. *J. Non-Newton. Fluid Mech.* **1986**, *21*, 79−97.
(35) Clasen, C.; Plog, J. P.; Kulicke, W.-M.; Owens, M.; Macosko, C.; Scriven, L. E.; Verani, M.; McKinley, G. H. How dilute are dilute solutions in extensional flows? *J. Rheol.* **2006**, *50*, 849−881.
(36) Muthukumar, M.; Freed, K. F. Theory of concentration dependence of polymer relaxation times in dilute solutions. *Macromolecules* **1978**, *11*, 843−852.
(37) Daoud, M.; Cotton, J. P.; Farnoux, B.; Jannink, G.; Sarma, G.; Benoit, H.; Duplessix, C.; Picot, C.; de Gennes, P. G. Solutions of flexible polymers. Neutron experiments and interpretation. *Macromolecules* **1975**, *8*, 804−818.
(38) Tirtaatmadja, V.; McKinley, G. H.; Cooper-White, J. J. Drop formation and breakup of low viscosity elastic fluids: Effects of molecular weight and concentration. *Phys. Fluids* **2006**, *18*, 043101.
(39) Zell, A.; Gier, S.; Rafaï, S.; Wagner, C. Is there a relationship between the elongational viscosity and the first normal stress difference in polymer solutions? *J. Non-Newton. Fluid Mech.* **2010**, *165*, 1265−1274.
(40) Bazilevskii, A. V.; Entov, V. M.; Rozhkov, A. N. Breakup of an Oldroyd liquid bridge as a method for testing the rheological properties of polymer solutions. *Polym. Sci., Ser. A* **2001**, *43*, 716−726.
(41) Merchiers, J.; Reddy, N. K.; Sharma, V. Extensibility-Enriched Spinnability and Enhanced Sorption and Strength of Centrifugally Spun Polystyrene Fiber Mats. *Macromolecules* **2022**, *55*, 942−955.
(42) Palangetic, L.; Reddy, N. K.; Srinivasan, S.; Cohen, R. E.; McKinley, G. H.; Clasen, C. Dispersity and spinnability: Why highly polydisperse polymer solutions are desirable for electrospinning. *Polymer* **2014**, *55*, 4920−4931.
(43) Malkin, A. Ya.; Semakov, A. V.; Skvortsov, I. Yu.; Zatonskikh, P.; Kulichikhin, V. G.; Subbotin, A. V.; Semenov, A. N. Spinnability of Dilute Polymer Solutions. *Macromolecules* **2017**, *50*, 8231−8244.
(44) Merchiers, J.; Slykas, C. L.; Martínez Narváez, C. D. V.; Buntinx, M.; Deferme, W.; Peeters, R.; Reddy, N. K.; Sharma, V. Fiber Engineering Trifecta of Spinnability, Morphology, and Properties: Centrifugally Spun versus Electrospun Fibers. *ACS Appl. Polym. Mater.* **2022**, *4*, 2022−2035.
(45) Merchiers, J.; Martínez Narváez, C. D. V.; Slykas, C. L.; Reddy, N. K.; Sharma, V. Evaporation and Rheology Chart the Processability Map for Centrifugal Force Spinning. *Macromolecules* **2021**, *54*, 11061−11073.

https://doi.org/10.1021/acs.macromol.3c00097
Macromolecules 2023, 56, 4919−4928

(46) Sitaramaiah, G.; Smith, C. L. Turbulent Drag Reduction by Polyacrylamide and Other Polymers. *SPE J.* **1969**, *9*, 183−188.
(47) Mungan, N.; Smith, F. W.; Thompson, J. L. Some Aspects of Polymer Floods. *J. Pet. Technol.* **1966**, *18*, 1143−1150.
(48) Lu, P.; Hsieh, Y.-L. Organic compatible polyacrylamide hydrogel fibers. *Polymer* **2009**, *50*, 3670−3679.
(49) Desai, K.; Kit, K. Effect of spinning temperature and blend ratios on electrospun chitosan/poly (acrylamide) blends fibers. *Polymer* **2008**, *49*, 4046−4050.
(50) Odell, J. A.; Keller, A. Flow-induced chain fracture of isolated linear macromolecules in solution. *J. Polym. Sci. B Polym. Phys.* **1986**, *24*, 1889−1916.
(51) Odell, J. A.; Keller, A.; Rabin, Y. Flow-induced scission of isolated macromolecules. *J. Chem. Phys.* **1988**, *88*, 4022−4028.
(52) Odell, J. A.; Muller, A. J.; Narh, K. A.; Keller, A. Degradation of polymer solutions in extensional flows. *Macromolecules* **1990**, *23*, 3092−3103.
(53) Park, N.; Umanzor, E. J.; Conrad, J. C. Aqueous Colloid+ Polymer Depletion System for Confocal Microscopy and Rheology. *Front. Phys.* **2018**, *6*, 42.
(54) Kulicke, W.-M.; Kniewske, R.; Klein, J. Preparation, characterization, solution properties and rheological behaviour of polyacrylamide. *Prog. Polym. Sci.* **1982**, *8*, 373−468.
(55) Papageorgiou, D. T. On the breakup of viscous liquid threads. *Phys. Fluids* **1995**, *7*, 1529−1544.
(56) Martínez Narváez, C. D. V.; Dinic, J.; Lu, X.; Wang, C.; Rock, R.; Sun, H.; Sharma, V. Rheology and pinching dynamics of associative polysaccharide solutions. *Macromolecules* **2021**, *54*, 6372−6388.
(57) McKinley, G. H.; Tripathi, A. How to extract the Newtonian viscosity from capillary breakup measurements in a filament rheometer. *J. Rheol.* **2000**, *44*, 653−670.
(58) Fardin, M. A.; Hautefeuille, M.; Sharma, V. Spreading, pinching, and coalescence: the Ohnesorge units. *Soft Matter* **2022**, *18*, 3291−3303.
(59) Chen, Y.-J.; Steen, P. H. Dynamics of inviscid capillary breakup: collapse and pinchoff of a film bridge. *J. Fluid Mech.* **1997**, *341*, 245−267.
(60) Day, R. F.; Hinch, E. J.; Lister, J. R. Self-similar capillary pinchoff of an inviscid fluid. *Phys. Rev. Lett.* **1998**, *80*, 704−707.
(61) Entov, V.; Hinch, E. J. M. Effect of a spectrum of relaxation times on the capillary thinning of a filament of elastic liquid. *J. Non-Newton. Fluid Mech.* **1997**, *72*, 31−53.
(62) Wolff, C. Molecular weight dependence of the relative viscosity of solutions of polymers at the critical concentration. *Eur. Polym. J.* **1977**, *13*, 739−741.

https://doi.org/10.1021/acs.macromol.3c00097
Macromolecules 2023, 56, 4919−4928